Utrecht University
Faculty of Geosciences
Department of Earth Sciences

ISSN 2211-4335

Mohamed M.A. Elkelani – Silurian and Devonian source rocks and crude oils from the western part of Libya

USES 71

71

Silurian and Devonian source rocks and crude oils from the western part of Libya

Organic geochemistry, palynology and carbon isotope stratigraphy

Mohamed M.A. Elkelani

UTRECHT STUDIES IN EARTH SCIENCES

3 Carbon isotope chemostratigraphy and palynology of Late Devonian black shales from the eastern Murzuq Basin, Libya

Mohamed M.A. Elkelani[1], Jaap S. Sinninghe Damsté[1,2], Philippe Steemans[3], Gert-Jan Reichart[1,2], Zwier Smeenk[4]

[1] *Utrecht University, Faculty of Geosciences, Department of Earth Sciences, Organic Geochemistry, Budapestlaan 4, 3584 CD Utrecht, The Netherlands.*
[2] *NIOZ Royal Netherlands Institute for Sea Research, P.O. Box 59, 1790 AB, Den Burg, The Netherlands.*
[3] *University of Liège, Paléobiogéologie, Paléopalynologie, Paléobotanique B-18, Sart Tilman, 4000 Liège, Belgium.*
[4] *Utrecht University, Marine Palynology and Paleoceanography, Laboratory of Palaeobotany and Palynology, Faculty of Geosciences, Department of Earth Sciences. Budapestlaan 4, 3584 CD, Utrecht, The Netherlands*

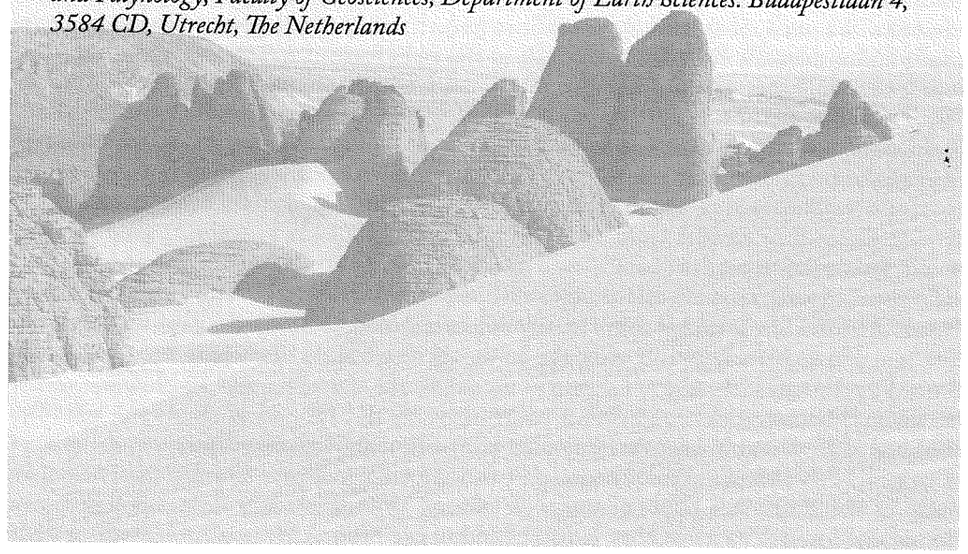

Abstract

In North Africa, several secondary source rocks have been suggested to contribute to known local oil reserves, in addition to the main Silurian age "hot" shale, source rock. It is, however, not clear from what age these potential source rocks would be and whether their contribution would come from appreciable in addition to the well-known major source rocks, which in Libya constitute the Tannezuft formation. One of the formations that was previously suggested to play a potential role in petroleum generation is the Awaynat Wanin formation, which is overlain by the Mrar formation. Therefore, the Awaynat Wanin and Mrar Formations from the eastern part of the Murzuq Basin in Libya were investigated using palynological, carbon isotopic and geochemical approaches. The sediments are from Late Givetian (Middle Devonian), Early Frasnian (Late Devonian) and Early Carboniferous ages. During the Frasnian organic-rich shales were deposited across much of the North African shelf, hence forming a potential secondary hydrocarbon source rock in this region. The high diversity of prasinophytes (e.g *Maranhites*, *Pterospermopsis*), high amount of organic matter and well preserved amorphous organic matter deposited during the early Frasnian strongly support enhanced sea surface productivity and oxygen-depleted bottom water conditions, possibly related to an expanding anoxic zone. Also, biomarker parameters indicate that the organic matter was derived from marine algal inputs and deposited under anoxic (reducing) conditions. Whole-rock carbon isotope analyses through the Awaynat Wanin formation revealed a positive $\delta^{13}C_{TOC}$ excursion, with a small 3‰ positive shift during the deposition of the Early to Middle Frasnian black shales. This excursion appears to be synchronous with a major positive $\delta^{13}C$ excursion previously recognized in northern Gondwana and eastern Laurussia. Increased tectonic activity, increased nutrient flux to the ocean, increased marine bioproductivity, widespread anoxia and related high organic carbon burial and regional relative sea-level rise are all likely factors responsible for the positive $\delta^{13}C_{TOC}$ excursion event. In other areas, this event resulted in the deposition of major amounts of potential source rocks. Although of more limited extent, Rock Eval and maturity data confirm that the early Frasnian black shale at the Late Devonian is potentially an effective source rock containing type II kerogen.

Key words: *Palynology, Carbon isotope, Rock Eval pyrolysis, Biomarker, Devonian, Frasnian black shales.*

1 Introduction

North African black shales form locally important source rocks for both oil and gas. The major source rock in this area, the so-called "hot" shale, was deposited during the Early Silurian (Klitzsh, 1963; Lüning *et al.*, 2000; see also Chapter 2). However, other (secondary) source rocks might have contributed to the formation of oil and gas. The marginal setting, with many semi-enclosed basins, probably remained prone to deposition of organic rich sediments for a major part of the geological past. During the Devonian, many of the Early Palaeozoic oceans were closing as Laurasia and Baltica collided into the newly formed continent of Laurussia. The northern African margin was at that

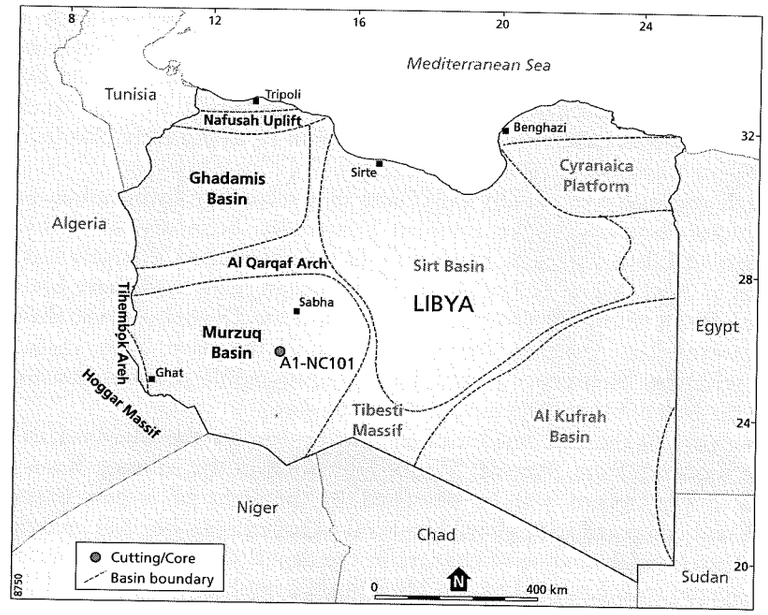

Fig. 1. Map showing the A1-NC101 well and geographic location of the Murzuq Basin.

time bordering the seaway separating Laurussia from the southern supercontinent of Gondwana (Bond *et al.*, 2004). The semi-enclosed nature of this seaway indicates that the Devonian was a time characterized by widespread black shale formation.

Particularly during the Frasnian (the early stage of the Late Devonian), black shales were deposited in many parts of North Africa. Thus they potentially form an important hydrocarbon source rock in this region. Time equivalent Frasnian organic-rich deposits in Europe occur, for example, in the Rhenish Massif/Harz Mountains (Germany) and the Montagne Noire (France). The organically richest and thickest Frasnian black shales are, however, deposited in central North Africa (Western Libya and Algeria). These black shales attracted much attention from researchers due to their association with major sea-level change, mass extinctions and their economic importance as a secondary source of hydrocarbons (Luning *et al.*, 2004; Wignall, 1991). The most famous of these shales was deposited during the so-called "Kellwasser Event", associated with a distinct transgression at the Frasnian-Famennian (F-F) transition. This event is also characterized by large-scale ocean anoxia and a major mass extinction (Walliser, 1996; Racki *et al.*, 2002). Deposits associated with this event have been identified globally in North Africa (Algeria and Morocco), Europe (e.g Germany, Great Britain, Poland, Portugal and Spain) and North America (Johnson *et al.*, 1985), although with a different sedimentary lithology. In general, during the Frasnian-Famennian mass extinction, about 15% of families and 50% of genera of marine fauna died out, and reefs almost completely disappeared (Riquier *et al.*, 2006). The mass extinction event appears synchronous with the deposition of black shales, which implies that conditions favored organic matter preservation (Joachimski

& Buggisch, 1993; McGhee, 2001). Several studies presenting detailed early and middle Frasnian (early Late Devonian) carbon isotope data from Poland (Racki *et al.*, 2004; Pisarzowska *et al.*, 2006; Yans *et al.*, 2007), Belgium (Yans *et al.*2007), and South China (Ma *et al.*, 2008) provide evidence that a major, long-lasting and widespread positive $\delta^{13}C$ isotope excursion occurred during the transition from the early Frasnian to middle Frasnian.

Although regionally potentially important as a secondary hydrocarbon source rock, detailed studies focusing on the Frasnian-Fammenian boundary are missing for the western parts of Libya, and their basin-scale facies distribution is largely unknown (e.g. Loboziak *et al* 1992; Mergl & Massa, 2000). Although many wells have been drilled in the Murzuq Basin studies focusing on the mid to Late Devonian black shale sequence lack age control. The Awaynat Wanin formation is the most likely candidate to be correlated with the "Kellwasser event", but its stratigraphic position remained unclear because of the lack of bio and chemo-stratigraphic data.

Here we present the first stable carbon isotope data for the Middle-Late Devonian black shale sequence from Awaynat Wanin Formation in the Murzuq Basin in western Libya. The $\delta^{13}C_{org}$ record will be discussed in the light of a new biostratigraphic framework and compared with global bio-events. Organic geochemical investigations are used for a better understanding of changes in the depositional environment of this black shale. The source rock potential of this black shale is evaluated using Rock Eval and its molecular composition.

2. Geological setting

The Murzuq Basin is a large intracratonic sag basin situated in the southwestern part of Libya, west of the Tibisti Massif (Fig.1). The basin extends into northern Niger, covering an area of about 330,000 km^2. The basin already formed early during the Paleozoic, acquiring its present shape through a succession of later tectonic activities. The basin is flanked on three sides by anticlines of Paleozoic strata, including the Al Qarqaf Uplift-Atshan Saddle to the north, the Tihemboka Arch in the west and Dor el Gussa-Jebal Mourizdie to the east (Aziz, 2000; Echikh & Sola, 2000).

The basin structure is characterized by normal faulting in an approximately NNW-SSE orientation. This normal faulting is thought to largely follow basement trends and led to the development of a prominent series of troughs and highs, such as the Serdeles trough, Tririne high and the Ubari trough (Aziz, 2000). The stratigraphic section of the basin is nearly 4000 m thick and is comprised of predominantly marine Paleozoic clastics, with some Mesozoic sediments of mainly continental origin (Belhaj, 1996). The stratigraphic section experienced varying degrees of erosion, mainly during the Caledonian, Hercynian and Alpine orogenies, although magnitude and timing of these events locally remains uncertain (Bellini & Massa, 1980). The Paleozoic section includes several organic-rich shale facies with petroleum source rock potential. These potential source rocks include the early Silurian (Llandoverian to Wenlockian) Tanezzuft Formation (the so-called "hot" shale), the Middle-Upper Devonian Awaynat Wanin, and the Lower Carboniferous Mrar Formations. In contrast to the Tannezzuft formation, the significance of the last two as effective source rocks in the Murzuq Basin has not

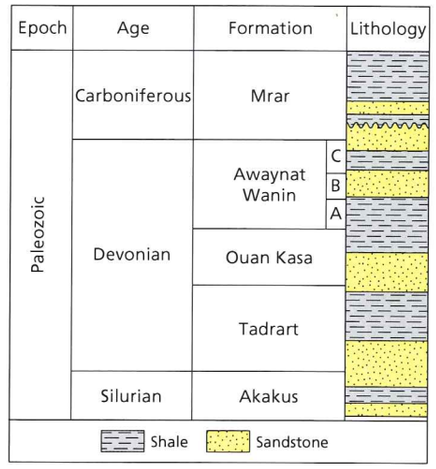

Fig. 2. Generalized stratigraphic column of the Murzuq Basin (modified after NOC, 2002)

been proven. Based on both outcrop and oil exploration wells drilled in the area, the Devonian sedimentary record in Libya has been divided into three formations (Fig. 2): Tadrart Formation, Ouan Kasa Formation, Awaynat Wanin Formation (A, B, and C) (Belhaj, 1996). The name Awaynat Wanin was introduced by Lelubre (1946), based on exposures on the western flanks of the Al Qarqaf Uplift. Such outcrops on the margins of the Murzuq Basin are, however, heavily weathered and oxidized and hence no longer suitable for organic biostratigraphic and organic geochemical studies. For that reason, we here concentrate on records drilled from the sub-surface.

3. Materials and methods

Concession NC101 was awarded to the Bulgarian Oil Company (BOCO) and drilled in 1980 (Fig. 1). The A1-NC101 borehole was positioned on the western flanks of the Traghan High to the south-east of Murzuq Basin (25°48 55 N 13°57 10 E). Repsol Oil Company provided 14 samples from this borehole-10 core samples and 4 cutting samples, together with infill cuttings from intervals between the cored sections. Unfortunately, no well log and gamma ray data are available. Core and cutting samples were retrieved from the interval between 2200 m to 2307.5 m depth, giving a total sampled thickness of 107 m. The samples were selected based on their shale contents, including green, grey and dark black shales (Table 1).

3.1. TOC and stable carbon isotope analysis

Total organic carbon content was determined using an elemental analyzer on decalcified samples. Samples were decalcified using 0.5 g of powdered material, which was allowed to react with 12 ml 1M HCl for 24 h. After decalcification, residues were washed with

demineralized water, centrifuged and decanted three times to remove acid-soluble components. Subsequently Total Organic Carbon (TOC) was determined using an elemental analyzer (Fisons NA 1500 NCS).

Sulfur content was measured on powdered whole rock samples using a LECO C/S SC632 analyzer with high-purity ceramic crucibles that had ultra-low sulfur content, and using standard instrument settings. One whole-rock sample from the most organic -rich rock from the Awaynat Wanin black shale formation from a depth of 2295 m was analyzed at the Royal Netherlands Institute for Sea Research (NIOZ). After complete destruction with an acid mixture of HNO_3, HF and HCl, the residue was taken up in HNO_3, before being measured on a Quadrupole ICP-MS (Thermo iCap) for Fe content.

Stable carbon isotope analysis of TOC was performed on 40-300 µg sub-samples of decalcified crushed rocks using an isotope ratio mass spectrometer (Thermofinnigan Delta Plus) coupled online to an elemental analyzer (Fisons NA 1500 NCS). Graphite Quartzite (GQ) was used as an internal standard and nicotinamide as a control. Results were normalized relative to Vienna Pee Dee Belemnite (VPDB) using international standards.

3.2. Rock-Eval pyrolysis

Pyrolysis analyses were carried out on a Rock Eval 6 pyrolysis instrument (Vinci Technologies SA, France) to evaluate the organic content and kerogen type of the samples. A crucible containing a small amount (100 mg) of crushed whole rock was introduced into a furnace at 300°C. The free hydrocarbons volatized at this temperature (S1) from the sample were quantified by a flame ionization detector (FID). The furnace temperature was then raised by 35 °C/minute to 600 °C. Within this temperature range the kerogen in the rock sample "cracks" produced further hydrocarbons (S2) and CO_2 associated with pyrolysis (300-390 °C) (S3). Parameters measured include volatile hydrocarbon content (mg HC/g rock, S_1), remaining hydrocarbon generative potential (mg HC/g rock, S_2), carbon dioxide yield (mg CO_2/g rock, S_3) and temperature of maximum pyrolysis yield (T_{max}). Source rock parameters such as Hydrogen Index (HI = S2/TOC*100), Oxygen Index (OI = S3/TOC*100), and Production Index (PI = S1/(S1+S2) were calculated from these measured values. Details on the Rock-Eval method and parameters as well as a summary of interpretive guidelines for Rock-Eval data are available in Espitalié *et al.* (1985).

3.3. Palynological and microscopical analysis

Eleven samples were selected for palynological analysis, with sample intervals varying according to the material available. For each sample ca, 15 g of shale were treated using standard palynological techniques. In short, samples were coarsely crushed with a pestle and mortar to pieces of about 5 mm, and then subjected to a 20% hydrochloric acid (HCl) treatment to dissolve carbonates. The samples were then allowed to stand until any reaction had stopped. After three washes with distilled water the samples were treated with 40% hydrofluoric acid (HF) to remove any silicate material and allowed to stand for at least 24 h, followed again by three washes with distilled water. No oxidation was performed on the organic residue. The size of the palynomorphs ranged from 5 µm

to > 200 µm. A 250 µm mesh sieve was used to remove oversized organic material. Subsequent sieving with a 10 µm mesh allowed the collection of the fraction containing palynomorphs. Because of the large amount of mineral residue still occurring in the samples after sieving, $ZnCl_2$ was applied to separate the lighter organic material from the heavier mineral particles such as pyrite. After that, a small part of the residue was mounted on a slide, embedded with glycerine jelly, covered and sealed with paraffin wax, allowing the palynomorphs to be studied using transmitted light microscopy.

3.4. Extraction and fractionation

A known weight (15-20 g) of powdered rock (core and cuttings; six samples in total), were used to extract lipids in a Soxhlet unit with an azeotropic solvent mixture of 200 ml of DCM/MeOH (9/1: v/v) for 24 h. Extracts were transferred to another round bottom flask to remove the anti-bumping granules and subsequently dried using a rotary evaporator until a few drops of solvent were left. These extracts were then transferred to a pre-weighed small vial and reduced to dryness under a stream of nitrogen. The vial with containing extract was weighed again to allow for quantification. When required elemental sulfur was removed from the extracts using activated copper, again drying the extracts under a stream of nitrogen and recording the weights before and after.

The total extracts were separated into apolar and polar fractions using short column chromatography on activated alumina by eluting with *n*-hexane/DCM (9:1, v/v), and MeOH/DCM (1:1, v/v) as solvents, respectively. The apolar fraction was subsequently separated into a saturated and aromatic fraction using an Ag^+-impregnated silica column, with n-hexane and a *n*-hexane/DCM (9:1) mixture, respectively.

3.5. Gas chromatography and gas chromatography-mass spectrometry (GC-MS)

The aliphatic and aromatic hydrocarbon fractions were analyzed by capillary column gas chromatography. Each fraction was dissolved in hexane to a concentration of about 1mg/ml of sample and 1 µl was injected. The fractions were run on a gas chromatograph (HP6890 series II) equipped with a CP-Sil 5 CB (Agilent) column (length 25 m, diameter 0.32 mm, film thickness 0.12µm), a FID for quantifying organic compounds and a flame photometric detector (FPD) to check for the presence of bound and/or elemental sulfur. Helium was used as a carrier gas, kept at constant pressure (100 kPa). Samples were injected on-column. The oven temperature was programmed from 70 to 130°C at 30 °C/min, from 130 to 320 °C at 4°C/min and kept at 320 °C for 20 min. The data was collected on a Lab Agilent chemstation data acquisition system. Aliphatic and aromatic fractions were analyzed and compounds were identified by GC/MS (Thermo, Trace GC Ultra), set at constant flow, using the same column and temperature programme as used for the GC analyses. Hopane (*m/z* 191) and steranes (*m/z* 217) were identified by comparison of mass spectra with previously published mass spectra. Because of co-elution, the concentration of phenanthrene, dibenzothiophene and methyldibenzothiophenes were determined by CG-MS analyses of the aromatic fractions using the ions mass m/z 178, 184, and 198, respectively.

4. Results

4.1. Biostratigraphy

The Awaynat Wanin Formation is considered to comprise the entire sequence between the top of the middle Devonian Ouan Kasa Formation (e.g. Loboziak *et al.* 1992; Streel *et al.* 1990; Boumendjel *et al.* 1988) and the base of the Carboniferous Mrar Formation (Fig. 2, Klitzsh, 1963). Dark grey to black shale recovered in the A1-NC101 borehole in the Murzuq Basin between 2300 and 2200 m in depth were, initially collected from the section by the national oil company. The assumption was that it represented the Silurian Tanezuft Formation ("hot" shale), which explains the ill-constrained local stratigraphy.

We investigated 11 palynological samples from the core and cutting samples, collected from the grey and dark black shales, because they are usually the most suitable for palynological study. The stratigraphic range of each palynomorphs and miospores taxon encountered in the section, and relative abundance of different palynological groups, are plotted in Fig. 3 and Plates I, II, III, IV, V, VI. Conodonts potentially allow high-resolution biostratigraphic dating of Early Paleozoic sediments. Conodonts, however, are not very frequent in shale-dominated succession, such as in the studied interval of core A1-NC101. Although in outcrops there sometimes still exists enough material to be collected for conodont stratigraphy, identification of the organic-rich intervals in outcrops is complicated, because the organic matter has often been oxidized due to weathering under Saharan arid conditions (Belhaj, 1996; Lüning *et al.*, 2004). Since conodont stratigraphy is not possible in the Murzuq basin well, biostratigraphy here is based on miospore and acritrach occurrences.

4.1.1 Miospore assemblages

In most samples, miospores are abundant and well-preserved, which suggests overall a relatively low thermal maturity. Down core occurrences for each miospore taxon encountered, as well as that of other palynological groups, are plotted in Fig. 3. Microscope pictures of typical examples of species are illustrated in Plates I and II. Using the down core occurrences, a time frame is developed based on the published miospore stratigraphy for the Awaynat Wanin formation through the basal Mrar Formation (Streel *et al.*, 1988).

The deepest samples between 2307 m and 2304 m contain *Geminospora lemurata, Grandispora protea,* and *Samarisporites eximius*. Based on the sedimentary log, these samples are considered to belong to the lower part of Awaynat Wanin Formation. This implies that the base of this formation is late Givetian to early Frasnian (Playford, 1983; Loboziak & Streel, 1995, 1998; Streel *et al.*, 1988, 1990).

The common miospores species recovered from laminated black shales (2297, 2295 and 2290 m) immediately above the lower Awaynat Wanin Formation boundary contain *Ancyrospora pulchra, Auroraspora* sp,. *Geminospora lemurata, Grandispora riegelii, Hystricosporites* sp., *Samarisporites triangulatus,* and *Verrucosisporites premnus,* a species typical of the Early Frasnian (Streel *et al.*, 1987; Melo & Loboziak, 2003). In line with the Amazon Basin the earliest representatives of *Samarisporties triangulatus* area also associated with, or immediately succeeded by, spores bearing a tabulate sculpture, such as

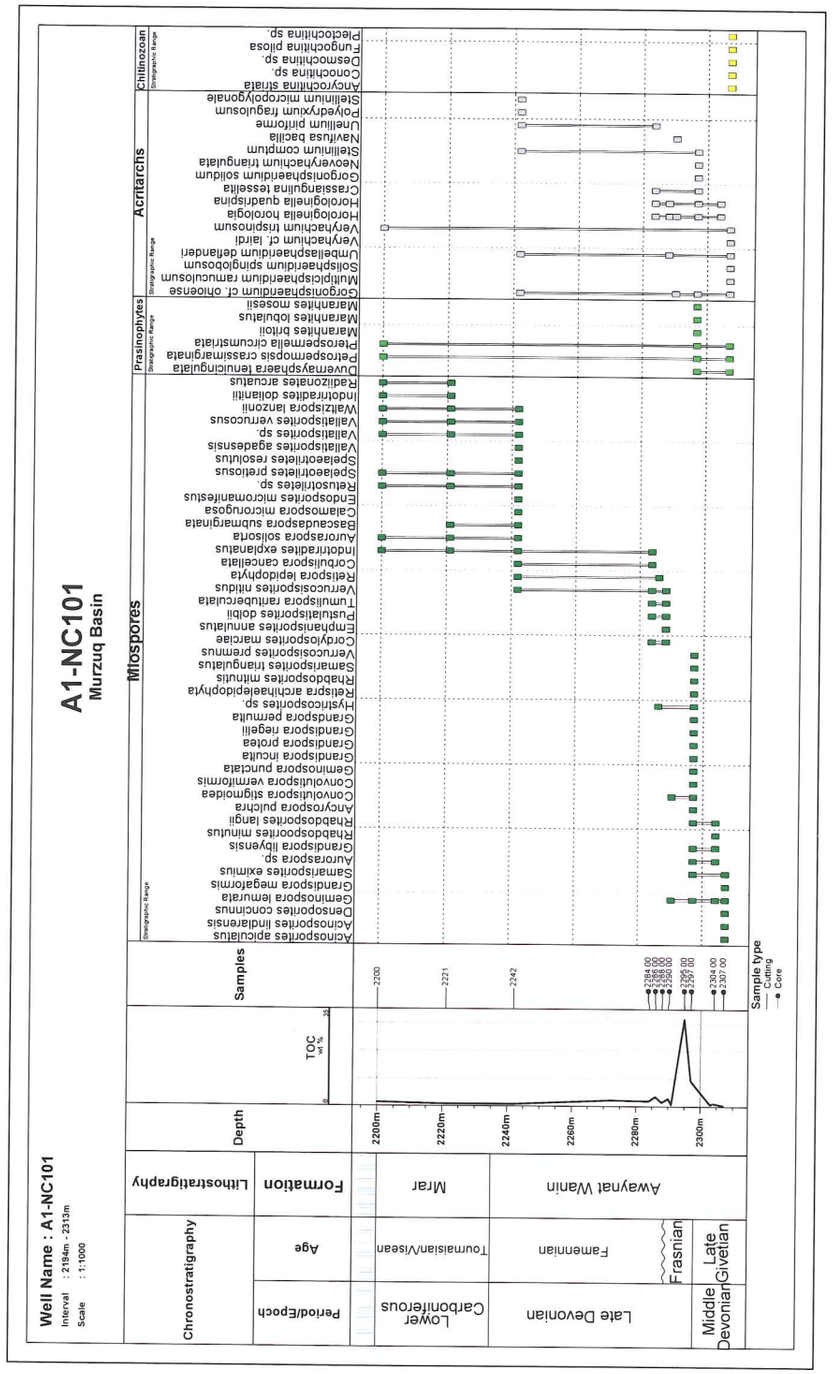

Fig. 3. Stratigraphic occurrence of miospore and palynomorhp range chart recorded samples of A1-NC101 borehole in the Murzuq Basin.

Geminospor, and *Verrucosisporites.* This implies that this section corresponds to Frasnian to late Famennian times.

The next miospore assemblage *Cordylosporites marciae, Indotriradites explanatus, Retispora lepidophyta, Tumulispora rarituberculata* and *Verrucosisporites nitidus,* occurs throughout the upper, less black shale containing, part of the record. This should correspond to the Latest Frasnian to late Famennian (Loboziak & Melo 2000; Melo & Loboziak 2003). In the Amazon Basin latest Famennian miospore assemblages are often characterized by the joint occurrence of *Indotriradites explanatus Retispora lepidophyta* and some *Tumulispora rarituberculata* (Loboziak & Melo, 2000).

Three cutting samples (2242, 2221 and 2200 m) were investigated from this borehole as well (Fig. 3 and Plates I). Caving, however, could induce contamination by rock fragments falling from the borehole walls, as no casing has been used. Still, palynological cutting samples potentially contain *in situ* material from the maximum depth reached by the drilling, mixed with palynomorphs from the open hole. In this case, the Lower Carboniferous assemblage is promptly distinguished from the Latest Devonian ones by an abrupt change in the composition of the palynoflora. This change is evidenced by the appearance of several species such as *Indotriradites explanatus, Spelaeotriletes pretiosus, Vallatisporites verrucosus,* and *Waltzispora lanzonii* of Late-middle to early-late Tournaisian age (Dreesen *et al.*, 1993). Visean palynofloras recovered from the investigated samples are generally characterized such as *Indotriradites dolianitii, Radiizonates arcuatus,* which corresponds to an Early Visean age (Loboziak & Streel, 1995; Melo *et al.*, 1999). As currently envisaged, our proposed scheme consists of a succession of more than 40 miospore species spanning in age from Middle Devonian to the Lower Carboniferous.

4.1.2. Acritrach and Prasinophyte assemblages

The acritarchs are long-ranging and of little biostratigraphic significance, except that the taxa present here include the marker species *Horologinella horologia, Horologinella quadrispina, Navifusa bacilla, Polyedryxium fragosulum, Stellinium micropolygonate, Stellinium comptum, Unellium piriforme,* and *Umbellasphaeridium deflandrei.*

All samples are characterized by high abundance, and moderately diverse acritarch assemblages. (Fig. 3 and Plates III, IV, V). Highest abundances of prasinophytes (mostly *Pterospermopsis, Maranhites, and Leiosphaeridia*) occur between 2297 and 2295 m depth. Maranhites species (particularly *Maranhites mosesii, Maranhites lobulatus and Maranhites britoi*) are common in the Frasnian, together with other characteristic taxa such as *Duvernaysphaera* sp., and *Umbellasphaeridium deflandrei* (Oliveira, 1997). These species were previously recorded in the early Frasnian of northwestern Argentina (Ottone, 1996) and Brazil (Quadros, 1988, 1999). Other important species that have been recorded in Frasnian assemblages also appear within this interval, including *Umbellasphaeridium deflandrei,* which has Frasnian occurrences in Algeria, Ghana, Brazil and Bolivia (Pérez Leyton, 1991).

4.1.3. Chitinozoan assemblages

Chitinozoan assemblages were only observed in the deepest sample, at 2307 m, in the lower part of the Awaynat Wanin Formation. The association at this depth contains

Fungochitina pilosa, Desmochitina sp., *Plectochitina* sp., *Ancyrochitina* sp., *and Conochitina* sp (Fig. 3 and Plate VI), which have been reported from the Middle Devonian of northeast Libya (Streel *et al.*, 1988; Hutter., 1979). Hence this is in line with both Miospore and Acritarch stratigraphy.

4.2. Total organic Carbon and Sulfur content

The TOC values range between 0.4 and 38.4% (Fig. 4A, and Table 1). Low TOC values (0.43 and 1.16%) are observed in the Givetian rocks of the lower Awaynat Wanin Formation (Middle Devonian), between 2307 m and 2303 m. An increase is noted corresponding to the lowermost Frasnian of the upper Awaynat Wanin Formation (Upper Devonian), which is characterized by high TOC values (from 9.3 up to 38.4%). Maximum TOC values identify the dark black shale interval (between 2297 and 2295 m in depth). A return to relatively low TOC values is observed during the Upper Famennian (upper Awaynat Wanin Formation) and Lower Carboniferous (Mrar Formation), with green to grey shales (average TOC of about 1.5%), except at 2286 m, where a TOC value up to 3.6% is recorded.

The TOC values are clearly correlated to the S% content. Total sulfur values range between 0.27 to 16.4 wt% (Fig. 4B and Table 1). The maximum sulfur content (16.4%) was observed during the Frasnian black shale (2295 m depth). Combining the data from the ICP-MS analyses for Fe (5.2 %) with the S data from the elemental analyzer (16.4 %), shows that the molar Fe/S ratio is over 5.

4.3. Rock- Eval pyrolysis data

The source rock properties of the Awaynat Wanin shales were investigated using Rock Eval pyrolysis, characterizing organic richness, hydrocarbon potential of the organic matter, kerogen type and thermal maturity (Fig. 5 and Table 1). The samples analyzed between 2286 and 2295 m have S_2 yields in the range of 7.7-181 mg HC/g rock. Frasnian black shale samples have high HI values between 236-472 mg HC/g TOC and low OI values, ranging from 3-31 mg CO_2/g TOC (Fig. 5, Table 1). T_{max} values are fairly uniform throughout the record, ranging from 438 to 442 °C.

4.4. Carbon isotopes

During the lower part of the record, i.e., the Givetian section, $\delta^{13}C_{org}$ values range between -27.0‰ to -26.0‰, which implies a+1‰ positive shift toward the Frasnian. During the Early Frasnian, the carbon isotope record (Fig. 4C Tabe 1) shows an appreciable increase in $\delta^{13}C_{org}$, with maximum values at 2295 m. The values around -24‰ imply a +3‰ positive shift from the base of the record. $\delta^{13}C_{org}$ values return to values of about -25.5‰ during the Late Frasnian, staying constant between 2286 and 2200 m throughout the rest of the record, from Famennian to Tournaisian (Lower Carboniferous).

Table 1. Sample description, total organic carbon, and Rock Eval pyrolysis parameters.

Well name	depth	Sample type	TOC	S%	δ13CTOC	Rock-Eval pyrolysis						
	m		wt %		(‰VPDB)	S1	S2	S3	Tmax	HI	OI	PI
						mgHC/g rock	mgHC/g rock	mgCO2/g rock	°C	mgHC/g TOC	mgC02/g TOC	–
A1-NC101	**2200**	**Cutting**	1.0	0.8	-25.64	0.10	1.43	0.23	441	142	23	0.06
	2221	**Cutting**	1.0	1.5	-25.66	0.04	0.62	0.08	435	63	8	0.06
	2242	**Cutting**	0.7	0.5	-25.68	0.05	0.37	1.45	438	56	220	0.13
	2272	**Core**	1.2	0.7	-25.90	0.07	0.93	1.85	440	78	154	0.07
	2284	**Core**	1.9	1.4	-25.71							
	2286	**Core**	2.4	2.8	-25.72	0.40	7.73	0.06	439	328	3	0.05
	2288	**Core**	1.4	1.0	-25.80							
	2290	**Core**	3.5	0.1	-25.08	0.92	11.14	0.13	430	316	4	0.08
	2291	**Core**	0.8	0.1	-25.54	0.20	1.98	0	438	236	0	0.09
	2295	**Core**	38.4	16.4	-24.16	17.16	181.38	1.69	442	472	4	0.09
	2297	**Core**	9.3	0.3	-25.97	0.06	0.75	0.11	440	208	31	0.07
	2303	**Core**	0.7	0.3	-25.93							
	2304	**Core**	1.2	1.2	-26.05	0.74	3.98	0.03	442	343	3	0.16
	2307	**Core**	0.4	3.4	-27.03							

TOC= Total Organc Carbon, **S%** = Sulfur content, **Carbon isotope (whole rock), S1**= Free hydrocarbon, **S2** = remaining hydrocarbon generative potential yield, **S3**= carbon dioxide **HI**= Hydrogen index = S2/TOC*100 , **OI**= Oxygen index S3/TOC*100, **Tmax** = Temperature of maximum pyrolysis yield, **PI**= Production index S1/(S1+S2),

Table 2. Aliphatic gas chromatography. ,aturity evaluation and palaeoenviroment data. parameters.

Well name	Depth	Sample type	Gas chromatography data					Maturity and paleoenviroment data			
	m		EOM	Pr/Ph	Pr/*n*-C17 Ph/*n*-C18		CPI	Ts/Ts+Tm	Homohopane index	C28/C29	DBT/P
			mg/g rock					m/z 191	m/z 191	m/z 217	(m/z 184, 178)
A1-NC101	**2200**	**Cutting**	37.3	0.76	0.33	0.50	0.90	0.27	0.10	0.43	
	2242	**Cutting**	31.2	1.00	0.31	0.41	1.01	0.26	0.09	0.41	
	2272	**Core**	46.8	3.94	0.32	0.48	0.87	0.27	0.09	0.43	
	2286	**Core**	37.2	3.46	0.13	0.08	1.02	0.52	0.12	0.48	
	2290	**Core**	54.9	1.31	0.43	0.14	1.12	0.60	0.13	0.70	
	2295	**Core**	129.6	1.61	0.47	0.11	1.15	0.59	0.13	0.79	0.03
	2304	**Core**	43.7	1.02	0.35	0.15	1.12	0.56	0.14	0.57	

EOM= Extractable organic matter, **Pr/Ph ratio** = Pristane/Phytane, **Ts/Ts+Tm** (*m/z* 191), (Ts) = C27 18α(H)-trisnorneohopane, (Tm)= C27 17α(H)-trisnorhopane, (Homohopane index (m/z 191) C35αβ (S+R)/(C31αβ+C32αβ+C33αβ+C34αβ+C35αβ(S+R), C28/C29 (m/z 217) C28αα/C29αα, DBT/P (m/z 184/m/z178), Dibenzothiophenes/Phenanthrene, Carbon preference index (CPI) = $CPI = \frac{1}{2}\left[\frac{C_{25}+C_{27}+C_{29}+C_{31}+C_{33}}{C_{24}+C_{26}+C_{28}+C_{30}+C_{32}} + \frac{C_{25}+C_{27}+C_{29}+C_{31}+C_{33}}{C_{26}+C_{28}+C_{30}+C_{32}+C_{34}}\right]$

4.5. Composition of hydrocarbon biomarkers

A representative gas chromatogram of the saturated hydrocarbon fraction showing the *n*-alkane (*n*-C_{15}+) and acyclic isoprenoid alkane distribution within typical Devonian and Carboniferous samples are displayed in Fig. 6, and values for geochemical parameters based on *n*-alkane and acyclic isoprenoid alkane distribution are given in Table 2. In the upper part of the record, the *n*-alkane distribution shows a high abundance of the short-chain (*n*-C_{15}-*n*-C_{20}) compound. The values of the carbon preference index values (CPI) for the C_{25} to C_{34} *n*-alkanes vary between 1.12 and 1.15 (Table 2). However, in the upper part of the section they are lower, ranging between 0.87 and 1.02.

Acyclic isoprenoids occur in high relative abundances, with pristane/phytane (Pr/Ph) ratios varying between 0.76 and 3.9. At all depths, the *n*-C_{17} is more abundant than pristane and *n*-C_{18} is more abundant than phytane. Distinct changes in the ratio of pristane to *n*-C_{17} and phytane to *n*-C_{18} are observed in the record (Table 2).

The distributions of triterpanes and steranes were studied using GC-MS by monitoring the ions *m/z* 191 and *m/z* 217 (Fig. 7). The tricyclic terpanes were either low or absent. All intervals studied show abundant pentacyclic triterpanes, as evidenced by the m/z 191 mass chromatograms (Fig. 7). The relative abundance of the C_{29} to C_{30} hopane is generally similar throughout the record. C_{27} 17α (H)-trisnorhopane (Tm) is dominant over C_{27} 18α (H) -22,29,30-trisnorneohopane (Ts) at 2200, 2272, 2286 and 2295 m, with Ts/Ts+Tm ratios ranging from 0.3 to 0.6 (Fig. 4D and Table 2). The samples from 2290 and 2304 m depths show Ts being higher than Tm. The homohopane distributions (Seifert and Moldowan, 1978) are dominated by the C_{31} homohopane and show decreasing abundances with increasing carbon numbers. The αβ-hopanes are more prominent than the βα-hopanes, while the 22S-isomers are more dominant than the 22R-isomers among the homohopanes (C_{31}-C_{35}). The observed range of homohopane index values is between 0.09 and 0.14, with the highest values corresponding to the Frasnian black shale (Figs. 4E and Table 2).

The distributions of the regular steranes (C_{27}, C_{28}, and C_{29}) are revealed by the *m/z* 217 mass chromatograms shown in Fig. 7. The distributions of C_{27}: C_{28}: C_{29} regular steranes for the analysed intervals are similar (C_{27} > C_{29} > C_{28}), and diasteranes are absent. The distributions of C_{27}, C_{28}, and C_{29} ααα (20R) and βαα (20R) steranes are similar throughout. The C_{28}/C_{29}-sterane ratio (Schwark & Empt, 2006) was calculated (Table 2) and plotted in Fig. 4F. This ratio shows values between 0.43 and 0.79, with an average of 0.56. No isomerized steranes (e.g. αββ20S) were identified.

Results of the analyses of the aromatic fraction from the Frasnian black shale (2295 m) are presented in Fig. 8A and Table 2. The relative abundances of phenanthrene (P), and dibenzothiophene (DBT), were determined using the trace of the summed mass fragments m/z 178, 184, and 198 (Hughes *et al.*, 1995), (Fig. 8B). The dibenzothiophene/phenanthrene (DBT/P) ratio is low (0.027).

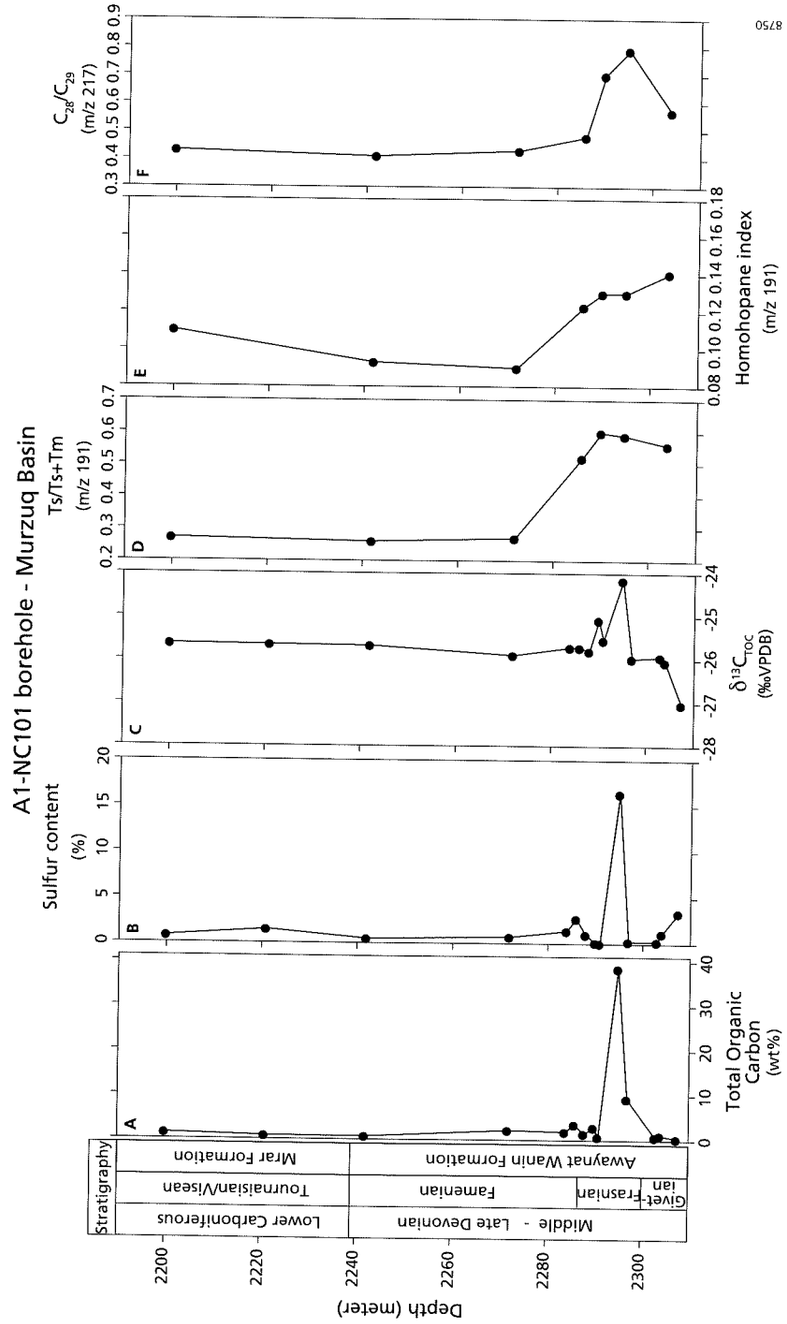

Figure 4. Stratigraphic patterns of biomarker proxies indicative of maturity and depositional environment. (A) total organic carbon (TOC), (B) sulfur content, (C) Ts/Ts+Tm (m/z 19, hopanes), (D) Homohopane index $C_{35}/(C_{31}+C_{35})$ (S+R) (m/z 19, hopanes), (E) C_{28}/C_{29} ααα20R (m/z 217, steranes), (F) Carbon isotope $\delta^{13}C_{TOC}$ from the whole rock

5. Discussion

5.1. Biostratigraphy and age model

The restricted stratigraphic distributions of most species encountered are in close agreement with what is known from other areas globally. The miospore taxa are taxonomically well established and allow for detailed age determination, which we used for establishing the age model. Although the acritarch taxa have much longer ranges, their occurrences are overall in good agreement with the miospore based age model (Fig. 3).

The stratigraphic interval from the Middle Devonian (Late Givetian) from the Murzuq basin yielded a relatively diverse and abundant chitinozoan-acritarch assemblage. Jardine and Yapaudjian (1968) showed similar species for the Middle Devonian (Late Givetian) acritarchs in the Algerian rock record. During the Middle Devonian the most age diagnostic species include *Geminospora lemurata* and *Grandispora libyensis*, a widespread Middle Devonian miospore species (Loboziak & Streel, 1995), which was first described. These form the Libyan Ghadamis Basin.

The Late Devonian assemblage is characterized by the occurrence of miospore species *Geminospora lemurata* and *Grandispora riegelii*, which all indicate an age not younger than Frasnian. Around the black shale interval *Gorgonisphaeridium* sp. is very abundant. The assemblage is dominated by the Praesinophyte species *Maranhites*, which is typical for the late Devonian assemblages in Bolivia, Brazil and Argentina (e.g., Ottone, 1996; Collbath, 1990; Limachi *et al.,* 1996; Le Hérissé & Deunff, 1988). Terrestrial components, such as plant miospores and tracheids, have a similar level or relative abundance throughout the investigated section, albeit being somewhat less abundant from 2297 to 2295 m.

The earliest Carboniferous assemblage is promptly distinguished from the latest Devonian ones by an abrupt change in the composition of the palynoflora. This change is evidenced by the appearance of species such as *Spelaeotriletes pretiosus, Vallatisporites verrucosus,* and *Waltzispora lanzonii,* which occur in the late Famennian to early late Tournaisian age (Dreesen *et al.*, 1993). *Indotriradites dolianitii* and *Radiizonates arcuatus,* occur in the Early Visean age (Loboziak and Streel, 1995; Melo *et al.*, 1999). The palynoflora also contains various holdovers of the latest Devonian-Tournaisian at the 2242 m interval. According to miospore data for the studied A1-NC101 borehole interval between samples at 2307 m to 2200 m, the timeframe is late Givetian to Lower Carboniferous.

The ratio of C_{28}/C_{29} sterane is considered a reliable age-related parameter for marine settings as it increases from Precambrian to Tertiary due to the relative increases of C_{28} sterane and decrease of C_{29} content through geologic time (Moldowan *et al.*, 1985). Therefore, it was possible for Grantham and Wakefield (1988) to distinguish Upper Cretaceous and Tertiary oils from Palaeozoic ones. In our rocks, the majority of the samples have a ratio < 0.7, which might be an indication for a source rock that is probably Palaeozoic in age. The sharp increase of the C_{28}/C_{29} sterane ratio (Fig. 4F) from 0.5 to 0.7 in the Devonian black shale implies a fundamental change in the green algae (e.g. *Pterospermopsis, Maranhites* and *Duvernaysphaera)* assemblage over time (Wignall, 1991; Schwark and Empt, 2006).

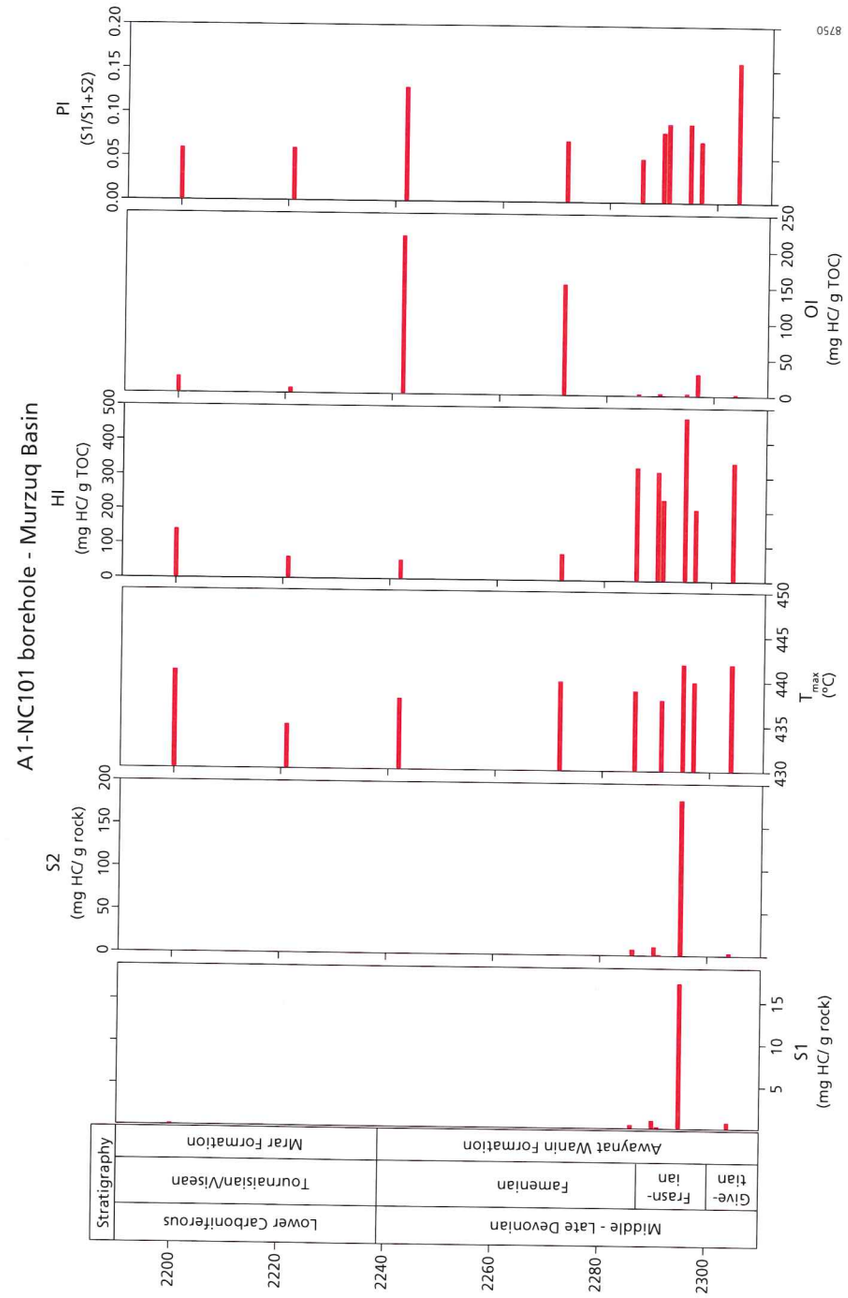

Fig. 5. Geochemical log from Rock Eval pyrolysis data of A1-NC101 borehole of Murzuq Basin

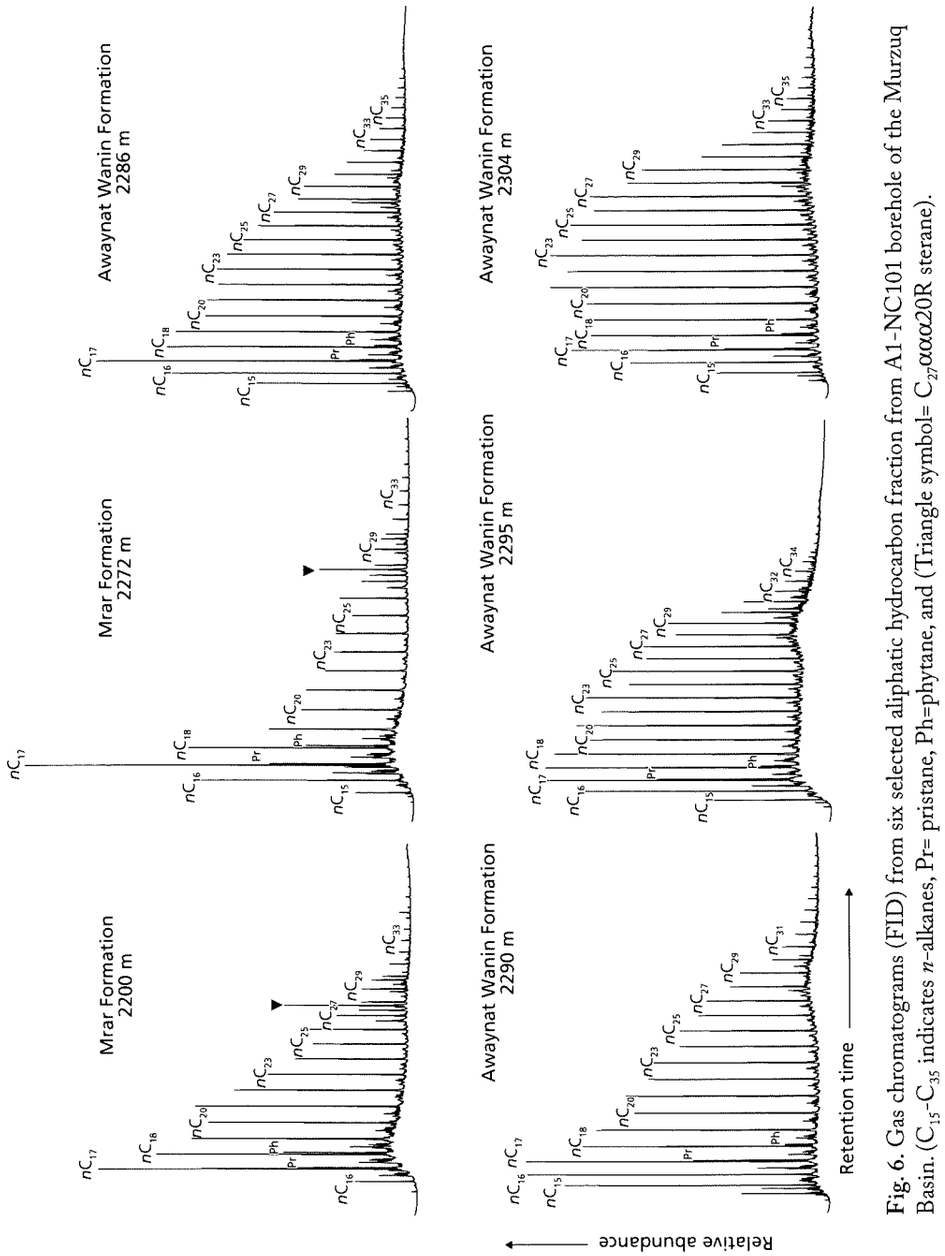

Fig. 6. Gas chromatograms (FID) from six selected aliphatic hydrocarbon fraction from A1-NC101 borehole of the Murzuq Basin. (C_{15}-C_{35} indicates *n*-alkanes, Pr= pristane, Ph=phytane, and (Triangle symbol= $C_{27}\alpha\alpha\alpha$20R sterane).

5.2. Stable carbon isotopic excursion

Our biostratigraphic results indicate that the observed excursion (Fig. 4C) to high $\delta^{13}C_{org}$ values in the Frasnian black shale in Awayant Wanin formation is time-equivalent to the globally observed isotope excursion during the early Frasnian. This excursion shows a maximum amplitude of around +7‰, representing the most prominent $\delta^{13}C$ excursion during the Devonian (Yans *et al.*, 2007). The isotopic excursion recorded in the Murzuq Basin has a smaller amplitude, but was measured on bulk organic carbon. Although compositional differences might have an influence on this $\delta^{13}C_{org}$ record (e.g. Sinninghe Damste & Köster, 1998), the relatively smaller amplitude of the excursion in Murzuq suggests that the complete event has not been captured. This might be due to the limited sample resolution in a relatively condensed sequence.

On a global scale, increased eutrophication and consequent enhanced organic carbon burial during the Early- Middle Frasnian transition has been invoked to explain the major positive carbon excursion (Racki *et al.*, 2004; Pisarzowska *et al.*, 2006). Global scale enhanced deposition of isotopically depleted organic carbon and resulted in an overall shift toward heavy values of the global exogenic carbon pool during the Frasnian. This is confirmed by the ubiquitous presence of Kellwasser black shales globally (e.g. Hangenberg black shale, Morocco, and Changshun Shale of South China), which provides evidence for a worldwide period of intensified accumulation of organic matter (Kump & Arthur, 1999). Also in the Murzuq, recorded elevated levels of OM burial (as judged from the elevated contents of TOC reaching almost 40%) coincide with the carbon isotopic excursion during the earliest Frasnian.

5.3. Conditions responsible for black shale deposition

The Frasnian black shale in the Murzuq Basin is characterized by unusually high TOC content, up to 38 wt % (Fig. 4A). This black shale is, however, relatively thin (~ 2 m). Both below, with organic carbon values during the late Givetian ranging from 0.16 to 0.36%, and above, with TOC values between 0.66 to 1.21% in the Lower Carboniferous, the TOC content is much lower than within the black shale. The black shale also has a high petroleum potential, with an S_2 >5 mg HC/g rock. The early Frasnian black shale interval also shows an interval of generally high HI and low OI values (Table 2). These high HI values, in combination with the high TOC content, suggest anoxic bottom water conditions and enhanced surface water productivity (Combaz, 1966; Revill *et al.*, 1994).

The sulfur content of the black shale is also relatively high, with atomic S/Fe ratios over 5, which implies that, at most, only a limited part of S is present in the form of pyrite. Microscopic observation revealed that some pyrites are present in the shales. Pyrite forms during early diagenesis when H_2S formed due to bacterial sulphate reduction, and reacts with iron(hydr)oxides to form iron monosulfides and ultimately pyrite (Berner, 1970). However, to stoichimetrically transform all formed H_2S to pyrite, enough iron(hydr)oxides are needed. When the water column is already oxygen depleted, the efficient transfer of iron(hydr)oxides is hampered and excess S can build up in the porewater, resulting in high S/Fe ratios. This free S could potentially bind to organic matter or be present as elemental S. The C/S ratio is often used to distinguish ancient euxinic environment, as iron-limited pyrite formation is often accompanied by high- sulfur and low-carbon values (Berner and

Raiswell, 1983), such as observed in the Black Sea. However, although the C/S ratio is rather low at about 2.3, the ratio between dibenzothiophene and phenanthrene (DBT/P), which is used to discriminate the impact of the depositional environment from the potential effect of source rock lithology (Hughes *et al.*, 1995), is 0.03, much lower than typical North Sea oil and Kimmeridge clay source rock showing values between 0.4 and 2.8 (Scotchman *et al.*, 1998). Hence most sulfur, with concentrations up to 16% (Figs. 4B and 8B), is probably present as inorganic sulfur.

The Pristane/Phytane (Pr/Ph) ratio can also be used to determine redox conditions of the sediment during deposition, based on the assumption that both pristane and phytane originate from the phytol side chain of chlorophll (e.g Didyk *et al.*, 1978; Powell, 1985), although the limitations of this approach have also been outlined (Ten Haven *et al.*, 1987). In the record studied here, ratios vary widely, between 0.76 and 3.9. The low values correspond to the Frasnian black shale, which is in line with the expected oxygen-depleted conditions during deposition. The higher values in the upper part of the record confirm reestablishment of oxic bottom water conditions after black shale deposition. Still the Pr/Ph ratio might also be affected by varying input of terrestrial organic matter. Changes therein are suggested by the *n*-alkane distribution, showing a distinct, albeit modest, odd-over-even carbon predominance from 2295 to 2290 m in depth (Fig. 6 and Table 2).

Homohopane distributions are dominated by the C_{31} homohopane, with decreasing relative concentrations with increasing carbon number (Fig. 7). The distribution of the extended hopanes or homohopanes (C_{31} – C_{35}) has also been used to evaluate redox conditions during deposition of source rocks, showing increased relative abundances of the C_{35} homohopane under anoxic conditions (Peters & Moldowan, 1991). Sinninghe Damsté *et al.*, (1995) showed that selective preservation of the C_{35} skeleton by sulfur incorporation is the most likely mechanism for the relative enrichment of the C_{35} homohopane under anoxic conditions. Still, at higher maturity levels the C_{35} homohopane potentially decreases again due to preferential generation of shorter-chain hopanes (Peters & Moldowan, 1991). Relative concentrations of the C_{35} hopane to the summed concentrations of the C_{31} to C_{35} hopanes >0.10 have been interpreted as indicative for deposition under anoxic bottom water conditions (Peters & Moldowan, 1991). This ratio for the samples analyzed here indicates that the Lower Awaynat Wanin Formation, with values ranging between 0.12 and 0.14, was deposited in a continuously anoxic environment. Although anoxic conditions might have extended into the water column, they most likely did not reach the photic zone (Sinninghe Damste *et al.*, 2001) as we did not detect any isorenieratene derivatives (Fig. 8A).

5.4. Thermal maturity assessment

The maturity level of the source rock was estimated by both by Rock Eval derived T_{max} values and by examining the hopane (m/z 191) distribution, specifically the Ts/Ts+Tm ratio. The Rock Eval T_{max} values range between 438 and 442 °C (Table 1). Although the maturation ranges of T_{max} values are known to vary for different types of organic matter (Espitalie *et al.*, 1985; Tissot *et al.*, 1987; Bordenave *et al.*, 1993; Peters, 1986), T_{max} values indicate that the organic matter has just reached the beginning of the oil window.

To distinguish between type and origin of the organic matter present, Rock Eval results can be plotted using a HI-T_{max} diagram (Fig. 9). Most of the Early Frasnian black

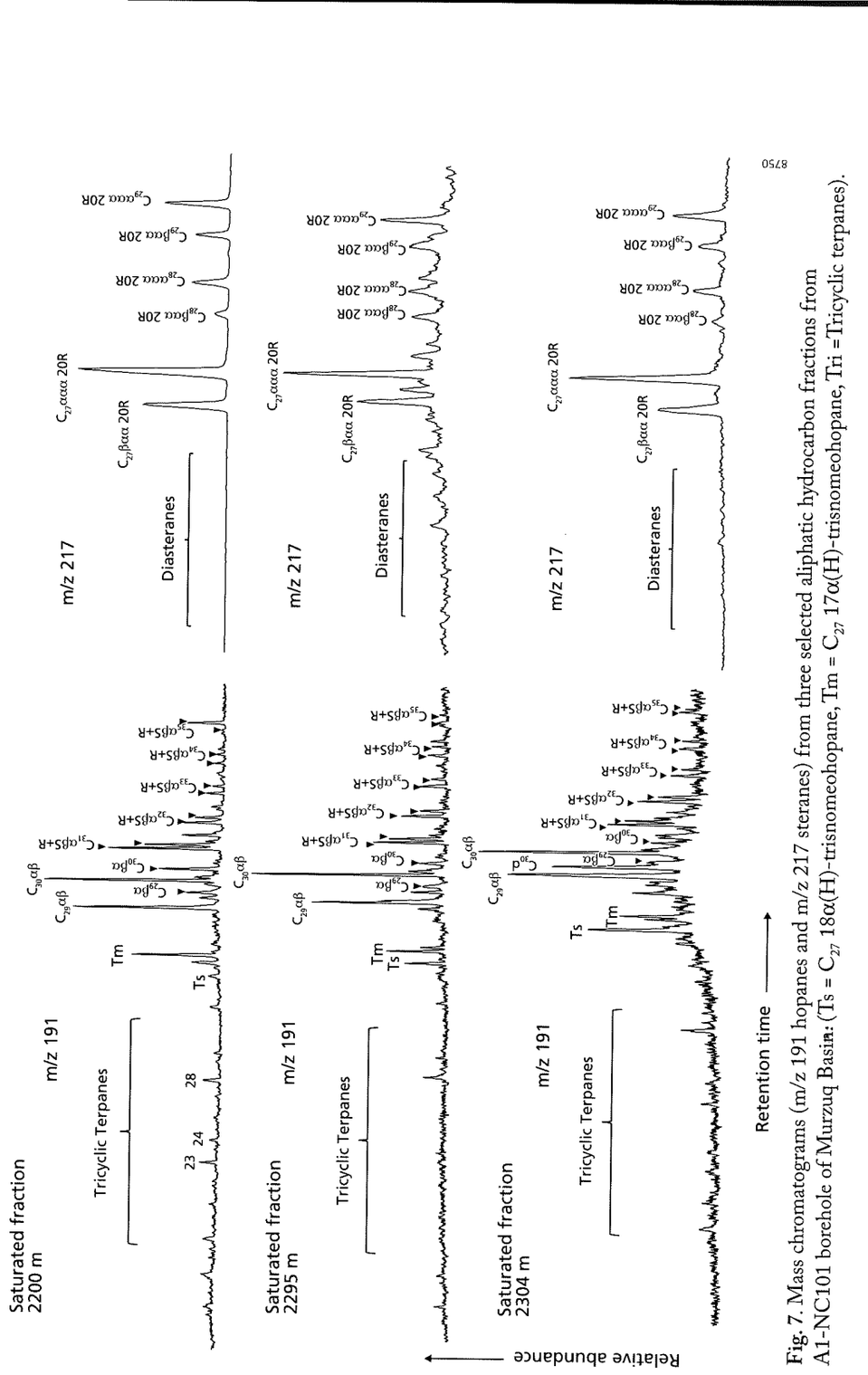

Fig. 7. Mass chromatograms (m/z 191 hopanes and m/z 217 steranes) from three selected aliphatic hydrocarbon fractions from A1-NC101 borehole of Murzuq Basin. (Ts = C_{27} 18α(H)-trisnomeohopane, Tm = C_{27} 17α(H)-trisnomeohopane, Tri = Tricyclic terpanes).

shale of the Awaynat Wanin plots in the Type II organic matter field (oil- and gas-prone), while the Carboniferous Mrar plots in Type III organic matter field (gas-prone) with low HI and S2 values. Similarly, based on hopanes it is also possible to evaluate source rock maturity, using the Ts/Ts+Tm ratio. This ratio is based on different thermal stabilities of these molecules (Seifert & Moldowan, 1978). The Ts/Ts+Tm ratio ranges between 0.59 and 0.60, which suggests that the Early Frasnian black shale attained a level of early maturity, in line with the Rock Eval Tmax data. The dominance of the ααα 20R steranes also indicates that the source rock is relatively immature (Peters *et al.*, 2005).

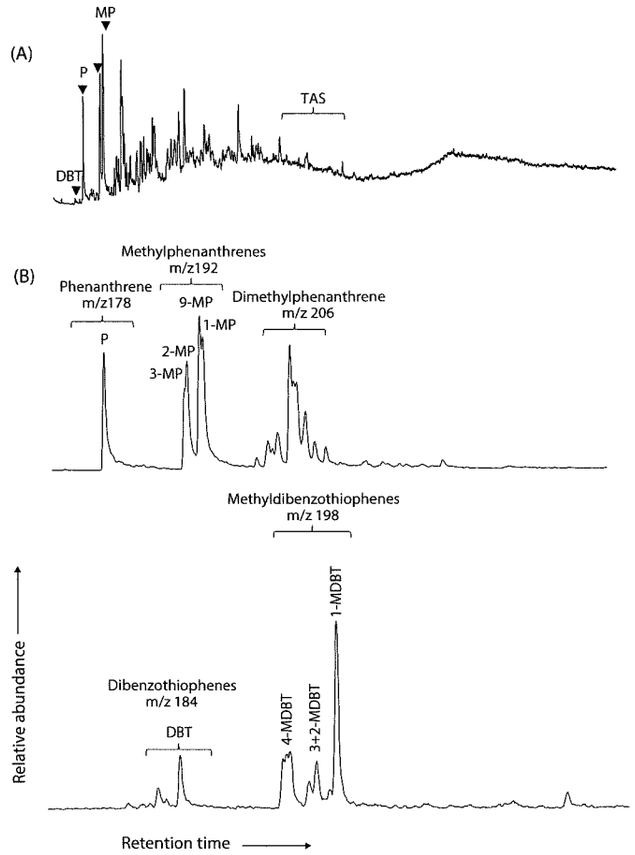

Fig. 8. Mass chromatograms from selected a sample (2295 m), (A) (TIC) of the aromatic hydrocarbon fraction, (B) and summed mass chromatogram of *m/z* 178+192+184+198, from A1-NC101 borehole (Murzuq Basin). Peak identification: P- phenanthrene; MP- methylphenanthrenes; DBT- dibenzothiophenes; MDBT- methyldibenzothiophene; TAS- triaromatic steroids.

5.5. Depositional model

Comparing the distribution of organics between the early Frasnian and the rest of the Devonian section shows that the AOM and *prasinophytes* are well-preserved. Although some supposedly terrestrial particles are present at these depths, the assemblage is overwhelmed by the marine prasinophytes *Pterospermopsis*, *Maranhites* and *Duvernaysphaera*. Palynofacies rich in AOM are often deposited under anoxic bottom water conditions (Tyson, 1993). At the same time the less diverse small acanthomorph acritarchs species indicate particular conditions at the sea surface. Similar acritarchs assemblages were observed in bituminous shales in the upper part of the Kowala section, in the Dasberg and Hangenberg intervals (Hartkopf-Fröder *et al.*, 2007; Marynowski *et al.*, 2010). Jardiné *et al.* (1974) studied the Late Devonian acritarchs of the Algeria rock records that showed great similarity to South America acritarch associations from the Frasnian. The paleogeographic setting, however, suggests a link to the Middle to Late Devonian onset of the collision between Laurentia and Gondwana. The relatively narrow nature caused by the gradual closure of the Iapetus Ocean would facilitate restricted conditions.

The Early Devonian in Libya is characterized by four transgressive sequences, which formed a widespread deltaic complex terminated by mid-Devonian uplift and erosion (Aziz, 2000). During the Middle to Late Devonian the gradual closure of the Iapetus

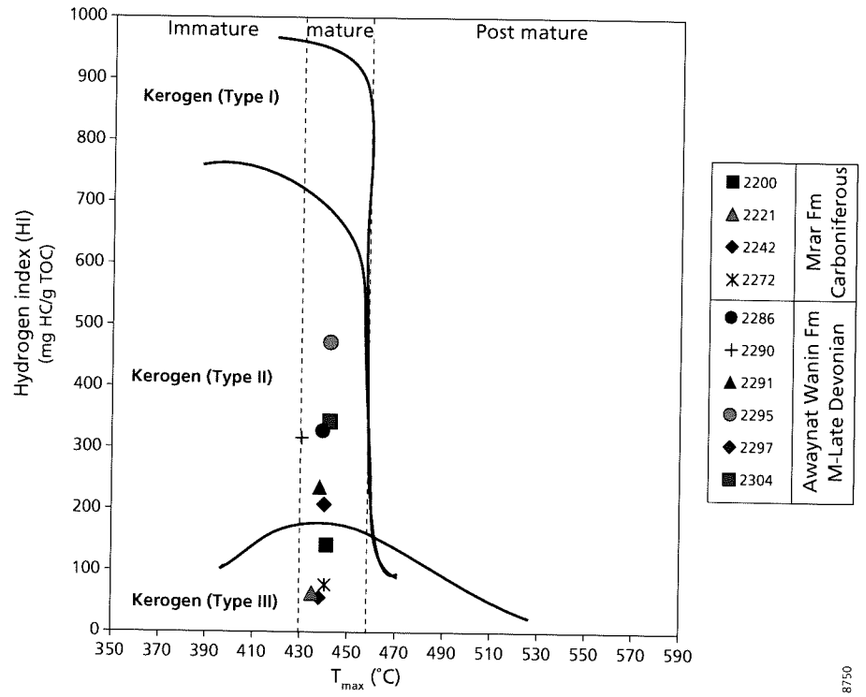

Fig. 9. Rock Eval Hydrogen index (HI) versus Tmax (°C) diagram of A1-NC101 borehole (Murzuq Basin), showing kerogen type and maturity evaluation.

Ocean brought progressive collision between Laurasia and Gondwana marking the onset of the Hercynian orogeny (Kent & Van der Voo, 1990). Initial effects of the closure were confined to Morocco and Algeria, with minor effects in Libya. Still, the basal Frasnian unconformity is caused by extensive erosion of the Al Qarqaf Arch (Boote *et al.*, 1998), which borders the Murzuq Basin.

The Frasnian unconformity was succeeded by a significant flooding event, during which organic-rich shales were deposited along the entire north Gondwana Margin (Luning *et al*, 2004). Although Buggisch and Joachimski (2006) and Morrow and Sandberg (2009) previously noted that not all positive excursions are associated with sea-level rise, the positive $\delta^{13}C_{org}$ recorded here appears to be closely timed with the onset of T-R cycle IIc.

The sediment deposited in Algeria and Morocco, however, contains much less organic carbon. While in the Murzuq basin the Frasnian black shale contains up to 38 wt% carbon, the Algerian Frasnian deposits contain up to 9 wt% organic carbon; in the bordering areas, most sediments contain even less organic matter. Clearly, conditions in the Murzuq Basin must have differed considerably. This not only affected preservation and production of organic matter, but also limited dilution with sediment. This is in line with the relatively limited thickness of the Frasnian black shales in Murzuq, which suggests a condensed section.

Uplift of the Al Qarqaf Arch, Tihemboka Arch and Atshan Saddle created ideal restricted depositional conditions in the Murzuq Basin. The highs surrounding the Murzuq Basin were probably still submerged, accumulating a thin Frasnian sedimentary sequence, which was removed during the later Hercynian uplift and erosion phase. More importantly, these uplifted areas effectively cut off the inputs of sediments from the Gondwana continent to the Murzuq Basin. The restricted oceanic conditions, in concert with enhanced weathering and nutrient inputs, set the stage for the deposition of organic rich sediments (Boote *et al.*, 1998). The limited input of terrestrial sediment in Murzuq enhanced these effects, explaining the unusual high organic carbon content.

6. Conclusions

Biostratigraphy of the organic-rich black shale of the Awaynat Wanin Formation showed that the recovered organic rich black shale from the eastern Murzuq Basin was deposited during the Early- Middle Frasnian/Late Devonian. This black shale is characterized by high TOC and sulfur contents. The abundant presence of marine amorphous organic matter, together with prasinophytes algae (*e.g. Maranhites, Pterospermopsis*) in this black shale in the Murzuq Basin, is in line with organic geochemical and biostratigraphic evidence for a strongly reducing depositional environment. The diversity of the prasinophycean and high concentration of organic matter also suggest enhanced surface productivity at the time of deposition. The onset of Frasnian black shale sedimentation is probably associated with the earliest Frasnian eustatic sea level rise, concurrent with a major positive $\delta^{13}C_{org}$ carbon isotope excursion of about 3‰. This positive excursion appears to be linked to the coeval deposition organic-rich black shales in Morocco, Algeria, Germany, Poland and South China. Although of limited extent, geochemical evaluation suggest that the Early Frasnian black shale, depending on its maturity, could be a potential secondary source rock for the Murzuq Basin.

Plate description and captions

Plate I. For each figured (miospore) specimen, sampling and slide number are indicated Scale bar is 10µm, except where mentioned otherwise.

1. *Vallatisporites* sp. (new speices), 2200, 2221, 2242 m, slide no. 1A, 2C, and 3A, X100
2. *Radiizonates arcuatus* Loboziak, Playford and Melo, 2000 (2200, 2221 m), slide no. 1A, 2C
3. *Waltzispora lanzonii*, Daemon 1974 (2200, 2221, 2242 m), slides no. 1A, 2C, and 3B, 60X
4. *Indotriradites dolianitii* (Daemon) Loboziak, Melo, Playford and Streel, 1999 (2200 m, 2221 m,), slide no. 1B, 2B.
5. *Spelaeotriletes pretiosus* (Playford) Neves & Belt, 1970 (2200, 2221, 2242 m), slides no. 1B, 2C, 3A
6. *Vallatisporites verrucosus,* Hacquebard, 1957 (2200, 2221, 2242 m), slide no. 1B, 2A and 3B
7. *Tumulispora rarituberculata* (Luber) Potonié, 1966 (2284, 2288 m), slide no. 4B, 5C, X40
8. *Retispora lepidophyta* (Kedo) Playford, 1976 (2284 m, 2288 m), slides no. 4A, 6B
9. *Verrucosisporites nitidus,* Playford, 1964 (2242, 2284, 2288 m), slide no. 3C, 4C, 6C

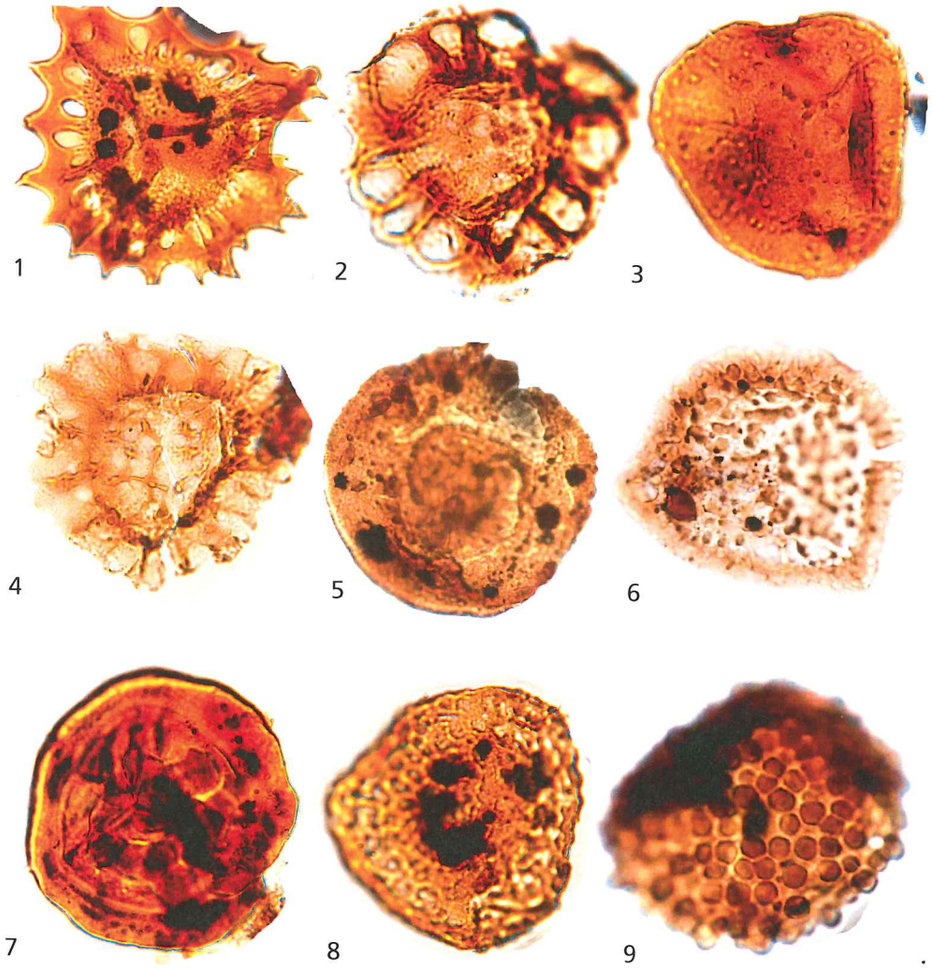

Plate. I (caption on page 96)

Plate II.

1. *Samarisporites triangulatus* Allen, 1965 (2297 m), slides no. 9A.
2. *Geminospora lemurata,* Balme emend Playford, 1983 (2290, 2297, 2304, 2307 m), slide no. 7A, 9C, 10A, 11D.
3. *Ancyrospora pulchra*, Owens, 1971 (2297 m), slide no. 9B.
4. *Samarisporites eximius* (Allen) Loboziak & Camfield, 1982 (2297, 2307 m) slide no. 9A, 11F
5. *Grandispora protea* (Naumova) Moreau-Benoit, 1980 (2297 m), slide no. 9B
6. *Hystricosporites* sp. Owens, 1971 (2286, 2297 m) slide no. 5B, 9A 60X
7. *Verrucosisporites premnus,* Richardson, 1965 (2297 m) slide no. slide no. 9A
8. *Grandspora libyensis,* Moreau-Benoit, 1980 (2297, 2304 m) slide no. 9B, 10B.
9. *Rhabosporites langii* (Eisenack) Richardson, 1960 (2297, 2304 m), slide no. 9C, 10A.
10. *Acinosporites lindlarensis,* Riegel, 1968 (2307 m), slide no. 11C
11. *Densosporites concinnus* (Owens) McGregor & Camfield, 1982 (2307 m) slide no. 11F, 11D

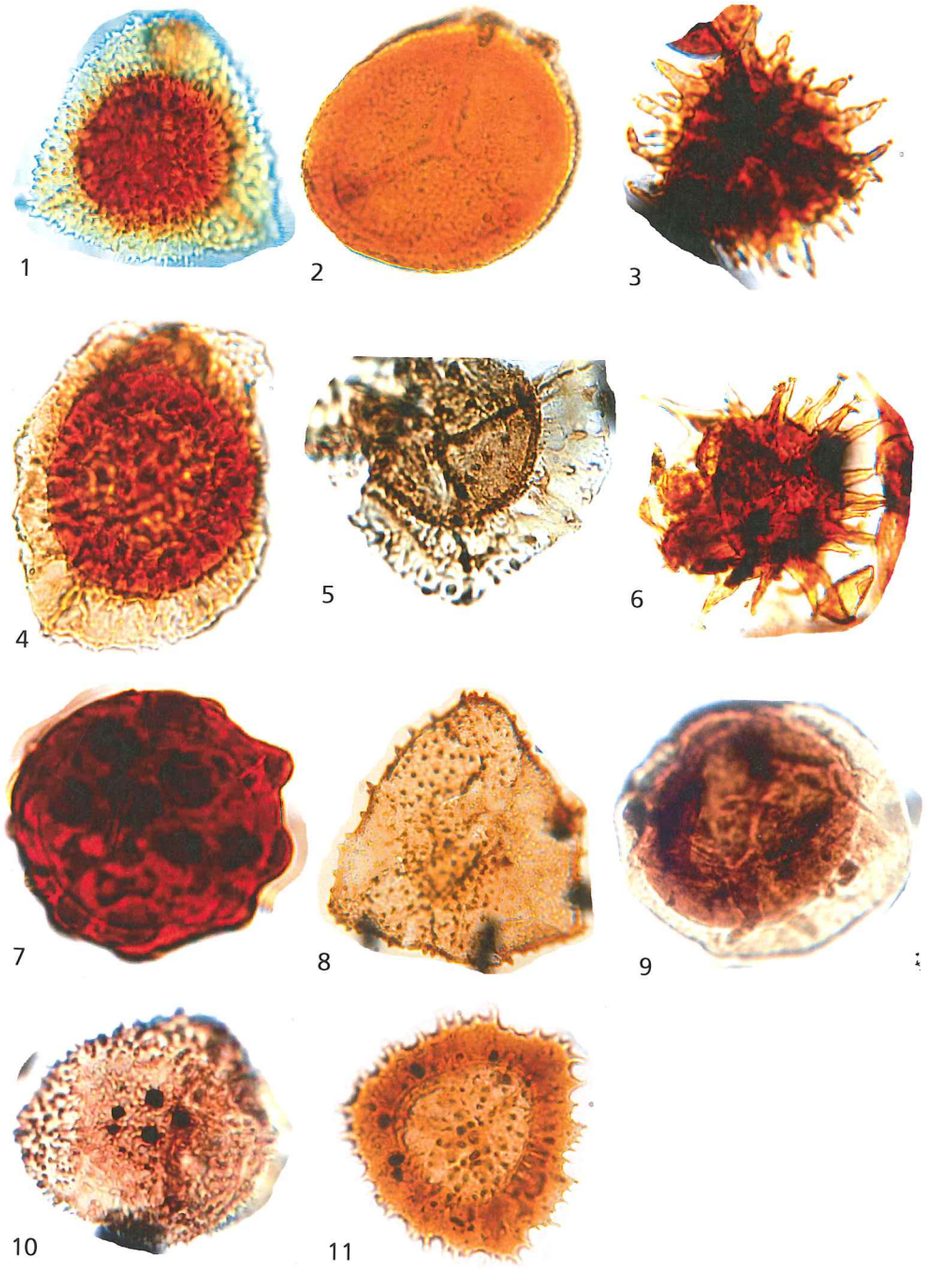

Plate. II (caption on page 98)

Plate III. Acritarchs and Prasinophytes (Scale bar 40µm see page) X600

1. *Stellinium comptum* Wicander & Loeblich, 1977 (2242, 2297 m), slide no. 3A, 9B.
2. *Stellinium micropolygonale* (Stockmans & Williere) Playford, 1977 (2242 m), slide no. 3C
3. *Horologinella horologia* Jardinė *et al*, 1972 (2284, 2288, 2297, 2290, 2304 m), slide no. 4C, 6B, 7D, 9C, 10C.
4. *Horologinella quadrispina* Jardinė *et al*, 1972 (2304, 2297, 2288, 2284 m), slide no. 10B, 9C, 6A, 4D.
5. *Maranhites lobulatus* Burjack & Oliveira, 1989 (2297 m), slide no. 9C, 9B, 60X
6. *Navifusa bacilla* (Deunff) Playford, 1977 (2290 m), slide no.7C, 7E

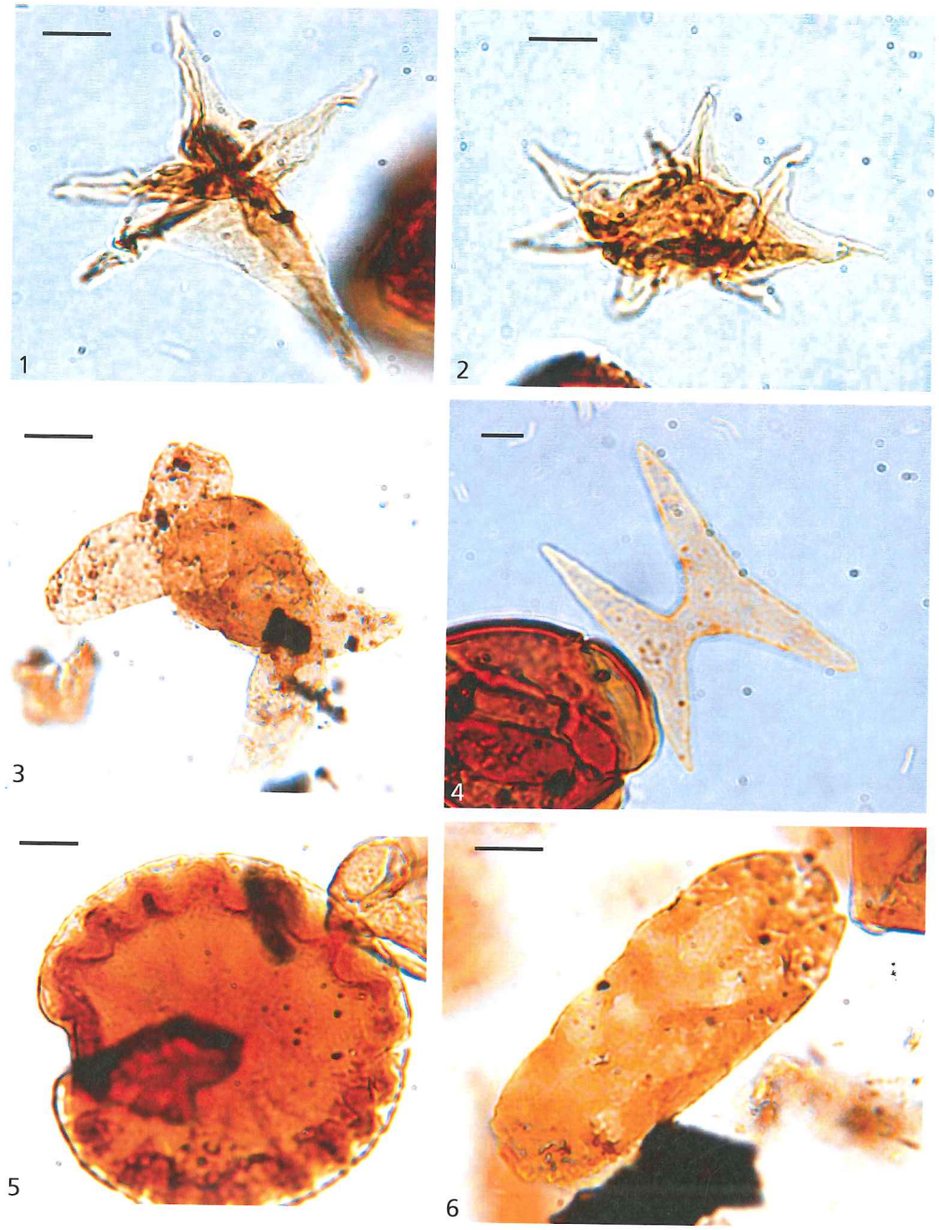

Plate. III (caption on page 100)

Plate IV.

1. *Unellium piriforme* Rauscher, 1969 (2242, 2286 m), slide no. 3A, 5B
2. *Crassiangulina tesselita,* Jardinė *et al.*, 1972 (2286 m, 2297 m), slide no. 9A, 5B
3. *Gorgonisphaeridium solidum,* Jardiné *et al*,1974 (2297 m), slide no. 9B
4. *Duvernaysphaera tenuicingulata*, Staplin, 1961 (2307, 2297 m) slide no. 11F, 9C.
5. *Umbellasphaeridium deflanderi* (Moreau-Benoit) Jardine *et al.*, 1972. (2307, 2288, 2242 m), slide no. 11C, 6B, 3C.
6. *Maranhites mosesii* (Sommer, 1965), Brito, 1967 (2297 m), slide no. 9C.

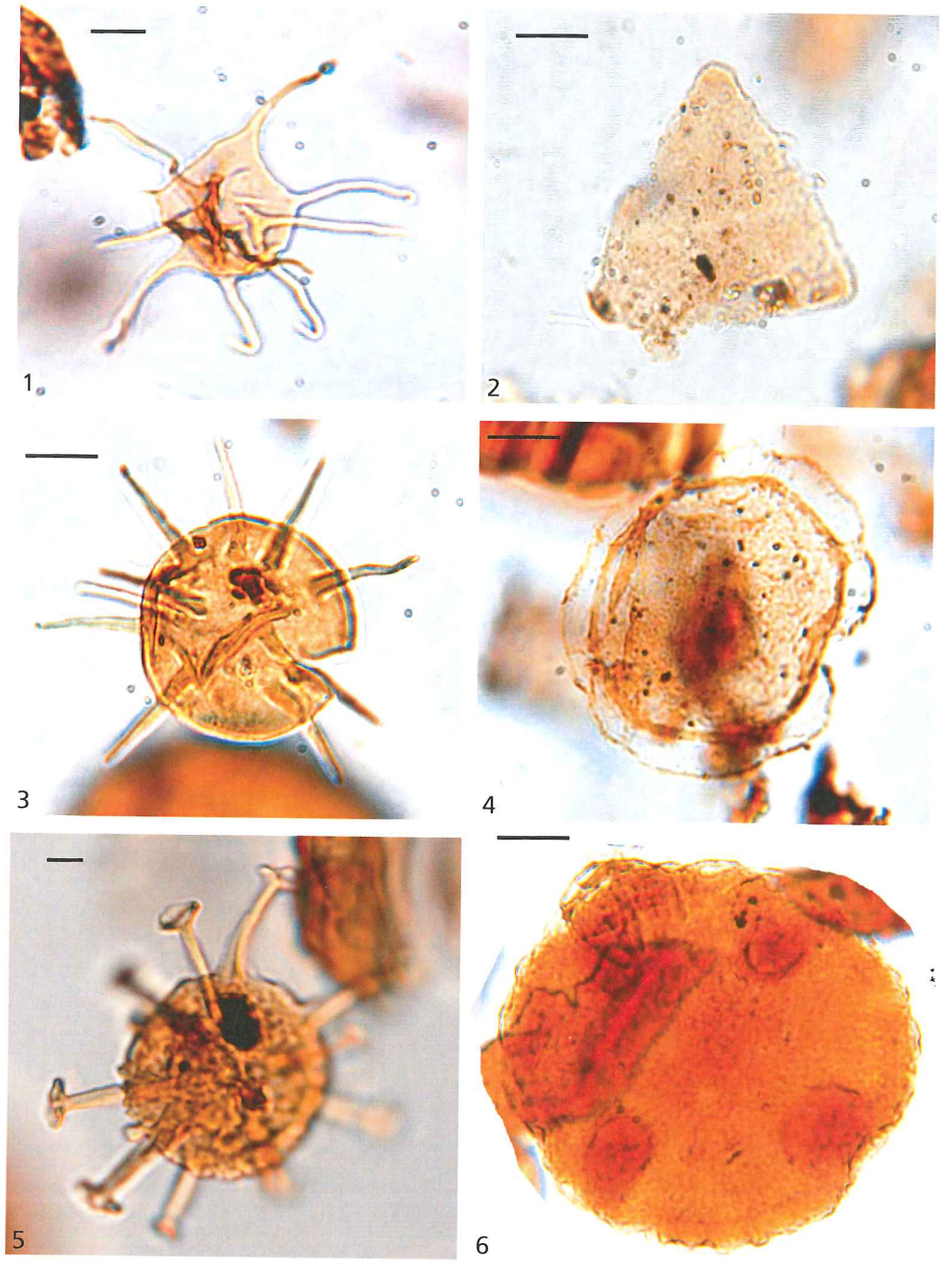

Plate. IV (caption on page 102)

Plate V.

1. *Neoveryhachium triangulate*, Le Hérissé, 1995 (2297m), slide no. 9B
2. *Veryhachium cf.V. lairdi,* Deunff, 1959 (2307 m), slide no. 11F
3. *Pterospermopsis Crassimarginata,* Oliveira, 2007 (2307. 2297, 2200 m), slide no. 1B, 9C and 11C
4. *Polyedryxium fragosulum*, Playford, 1977 (2242 m), slide no. 3B
5. *Gorgonisphaeridium ohioense,* (Winslow) Wicander, 1974 (2242, 2288, 2297, 2304 m), slide no. 3B, 6C, 9B, 10C.
6. *Solisphaeridium spinoglobosum*, (Staplin) Wicander, 1974 (2307 m), slide no. 11F

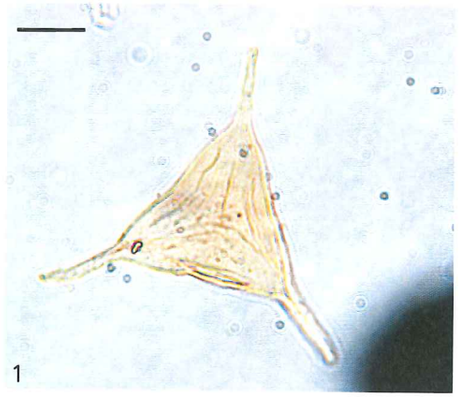
1

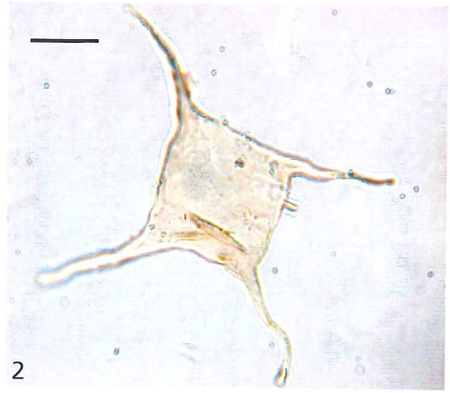
2

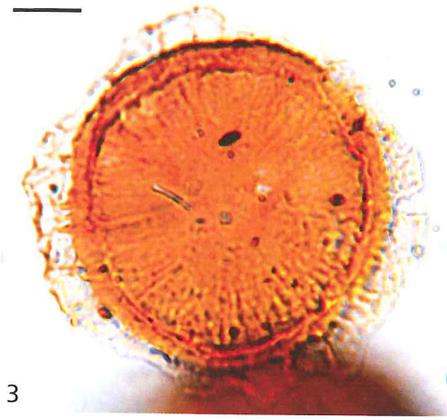
3


4

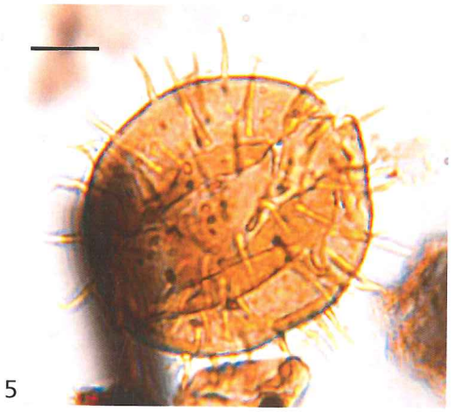
5

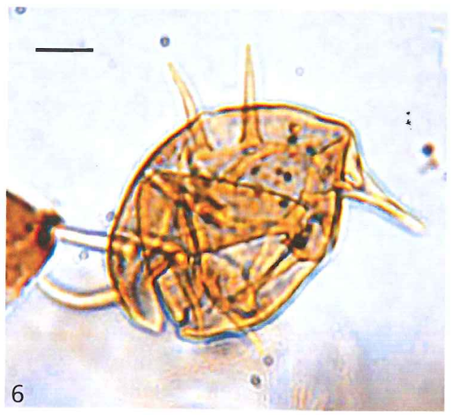
6

Plate. V (caption on page 104)

Plate VI. Chitinozoans, Amorhouse, Phytoclasts (Scale bar 40µm see page) X100

1. *Fungochitina fenestrate*, Taugourdeau & Jekhowsky, 1960 (2307 m), slide no. 11B
2. *Fungochitina pilosa* Collinson & Scott, 1958 (2307 m), slide no. 11F
3. *Urochitina* sp. A Jardiné & Yapaudjian 1968 (2307 m), slide no. 11D, 60X
4. *Ancyrochitina striata* Taugourdeau, 1963 (2307 m),slide no. 11B
5. Amorphous organic matter (AOM) (2295 m), slide no. 8A,B,C,D,F
6. Fluorescent light view of structureless, partly fluorescent well preserved AOM from black shale (2295 m).
7. Biostructured phytoclast Tyson, 1995 (2286, 2242 m), slide no. 3B,A, and 5A
8. Opaque biostructured phytoclast Tyson, 1995 (2286, 2242 m), slide no.. 3A, 5B.

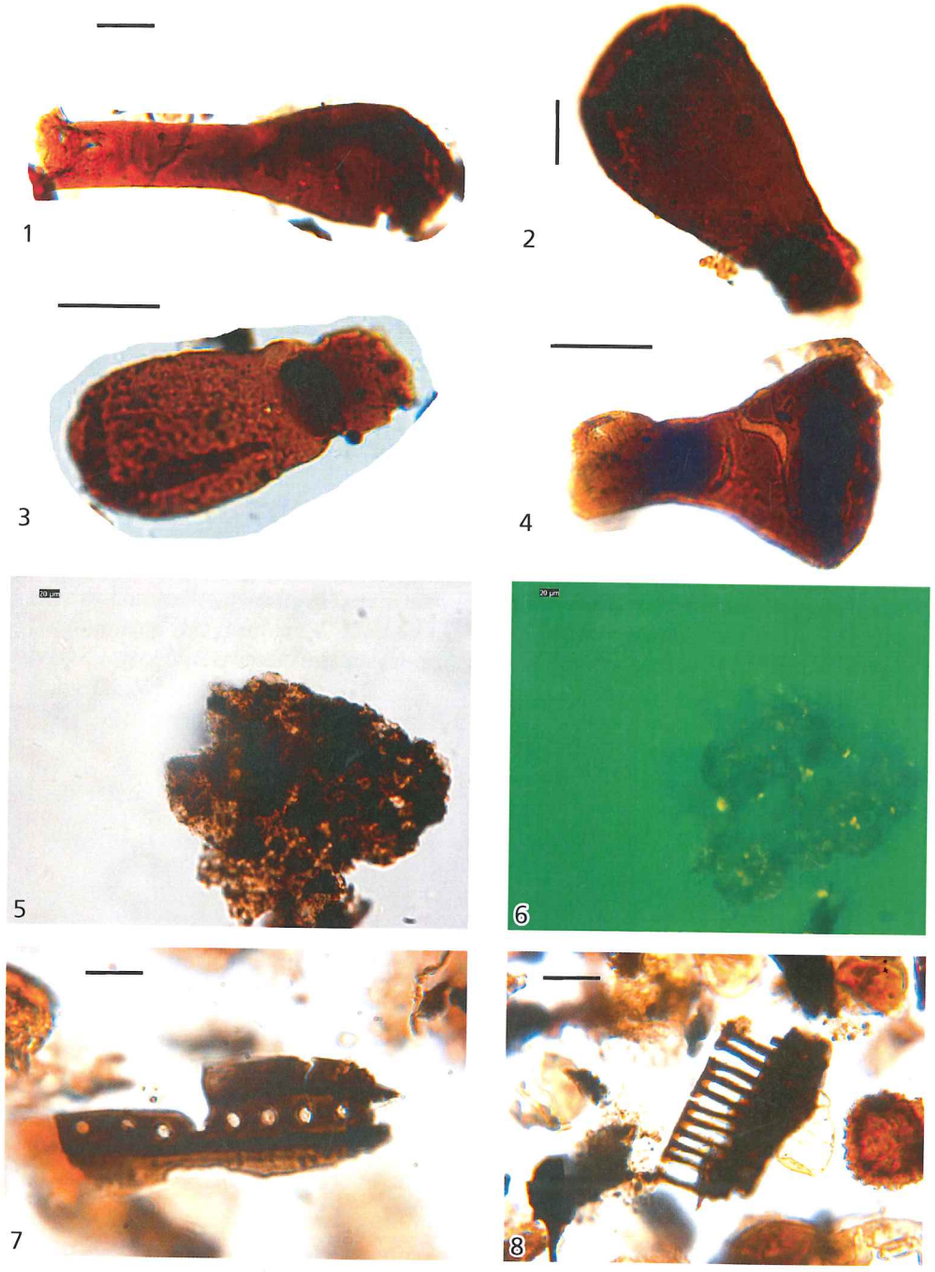

Plate. VI (caption on page 106)